

10. V. F. Castellucci, E. R. Kandel, T. E. Kennedy, P. Goelet, *Soc. Neurosci. Abstr.* **13**, 390 (1987).
11. C. H. Bailey and M. Chen, *Science* **220**, 91 (1983); *Soc. Neurosci. Abstr.* **12**, 1340 (1986).
12. For all experiments, we used $10^{-4}M$ cAMP analog (ICN), plus $5 \times 10^{-4}M$ IBMX (Sigma). By itself, this concentration of analog failed to produce either short- ($n = 3$) or long-term ($n = 3$) facilitation. Higher concentrations of cAMP analog could not be used because they caused the normally silent sensory neurons to become spontaneously active and fire action potentials.
13. Cultures were prepared by methods in (3), (4), and (8). The motor cell was impaled with an intracellular electrode filled with 1.5M KCl and held with hyperpolarizing current injection at 30 mV below the resting potential. The sensory neurons were stimulated with brief (0.2 to 0.4 ms) depolarizing pulses with an extracellular electrode filled with perfusion medium (equal volumes of Leibovitz's L-15 culture medium adjusted for marine saline conditions and artificial seawater plus *Aplysia* hemolymph to a final concentration of 2.5%). After the initial recordings of the EPSP, the cells were perfused with medium containing control or experimental drug treatments and maintained at 19°C. The cells were then rinsed in perfusion medium, returned to normal culture medium consisting of equal volumes of *Aplysia* hemolymph and L-15 medium, and placed back into the incubator at 18°C. The cells were reexamined 24 hours later with the same procedures.
14. B. Hochner, O. Braha, M. Klein, E. R. Kandel, *Soc. Neurosci. Abstr.* **12**, 1340 (1986).
15. D. Piomelli *et al.*, *Nature* **328**, 38 (1987).
16. An overall analysis of variance indicated a difference with treatment ($F = 6.14$, $df = 2,13$, $P < 0.025$). A comparison of the means (Dunnnett's test) indicated that treatment with phorbol ester did not differ from the control, whereas treatment with arachidonic acid significantly decreased EPSP amplitude compared to the control ($t = 2.86$, $P < 0.05$), or phorbol ester ($t = 2.54$, $P < 0.05$).
17. S. M. Greenberg, V. F. Castellucci, H. Bayley, J. H. Schwartz, *Nature* **329**, 62 (1987).
18. K. P. Scholz and J. H. Byrne, *Soc. Neurosci. Abstr.* **13**, 390 (1987).
19. ———, *Science* **240**, 1664 (1988).
20. D. L. Alkon, *ibid.* **226**, 1037 (1984); M. S. Livingstone, *Proc. Natl. Acad. Sci. U.S.A.* **82**, 5992 (1985); J. Farley and S. Auerbach, *Nature* **319**, 220 (1986).
21. J. H. Schwartz, V. F. Castellucci, E. R. Kandel, *J. Neurophysiol.* **34**, 939 (1971).
22. M. F. Miles *et al.*, *J. Biochem.* **256**, 12545 (1981); R. A. Maurer, *Nature* **294**, 94 (1981); G. Mangiarotti, A. Ceccarelli, H. F. Lodish, *ibid.* **301**, 616 (1983); M. Waterman, G. H. Murdoch, R. M. Evans, M. G. Rosenfeld, *Science* **229**, 267 (1985).
23. We thank R. Woolley for technical assistance; A. Krawetz for typing the manuscript; members of the Howard Hughes Medical Institute Mariculture Facility for providing the animals; and J. Byrne, N. Dale, M. Klein, P. G. Montarolo, K. Scholz, and J. Schwartz for comments on the manuscript. Supported by the Howard Hughes Medical Institute (E.R.K.), the McKnight Foundation (S.S.), and NIH grant GM 32099 (S.S. and V.F.C.).

19 January 1988; accepted 13 April 1988

Tandem Array of Human Visual Pigment Genes at Xq28

DOUGLAS VOLLRATH, JEREMY NATHANS, RONALD W. DAVIS

Unequal crossing-over within a head-to-tail tandem array of the homologous red and green visual pigment genes has been proposed to explain the observed variation in green-pigment gene number among individuals and the prevalence of red-green fusion genes among color-blind subjects. This model was tested by probing the structure of the red and green pigment loci with long-range physical mapping techniques. The loci were found to constitute a gene array with an approximately 39-kilobase repeat length. The position of the red pigment gene at the 5' edge of the array explains its lack of variation in copy number. Restriction maps of the array in four individuals who differ in gene number are consistent with a head-to-tail configuration of the genes. These results provide physical evidence in support of the model and help to explain the high incidence of color blindness in the human population.

COLOR BLINDNESS IS A COMMON trait in humans. Approximately 1 in 12 Caucasian males and 1 in 200 females are color-blind (1). The vast majority of color blindness is the result of alterations in the genes encoding the red and green visual pigments located at the end of the long arm of the X chromosome (2). The physical distance between these genes is not known, but the fact that they are 98% identical in DNA sequence suggests they arose by an evolutionarily recent duplication

event. Normal individuals possess from one to three green pigment genes but show no variation in the number of red pigment genes, which is always one (3). Examination of the structure of these loci in individuals with red or green color blindness revealed rearrangements of at least one of the genes in 24 of 25 cases (2). All of these rearrangements appeared to arise from homologous recombination, resulting in either a complete gene deletion or the production of fusion genes. This situation contrasts with that of other loci such as clotting factor VIII, ornithine transcarbamylase, and hypoxanthine-guanine phosphoribosyltransferase in which 2, 7, and 18%, respectively, of observed mutations are rearrangements and

most or all of these are intragenic deletions (4-6).

A model for the arrangement of the red and green visual pigment genes has been proposed to explain these observations (3). It specifies a head-to-tail tandem array of genes composed of the red pigment gene at the 5' end with a variable number of green pigment genes 3' to it. Homologous but unequal crossing-over in the array can generate the variation in green pigment gene number observed in normal subjects as well as the gene fusions and deletions observed in color-blind individuals. The fact that an entire red pigment gene is never duplicated or deleted is explained in this model by its position at the 5' end of the array, abutting unique sequences.

The model makes several specific predictions about the structure of the visual pigment loci as a function of the number of genes possessed by an individual (see below). These predictions could be experimentally tested by DNA physical mapping methods if the red and green pigment genes were sufficiently close together. To assess the distance between the two genes, very high molecular weight DNA prepared from the peripheral blood leukocytes of a normal male with one red and one green pigment gene was digested with restriction enzymes that cleave infrequently in the human genome. The digested DNA was fractionated on the basis of size by means of alternating contour-clamped homogeneous electric field (CHEF) gel electrophoresis, transferred to a membrane, and hybridized with a complementary DNA (cDNA) probe for the red pigment gene (Fig. 1) (7, 8). Because of the high degree of similarity between the genes, this probe detects the green pigment gene as well.

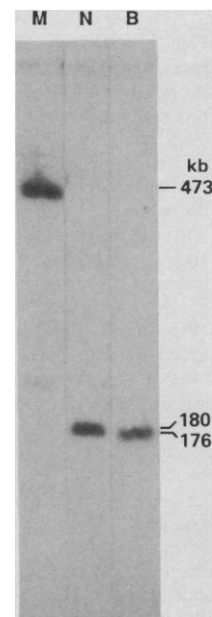


Fig. 1. Physical linkage of the red and green visual pigment genes. Very high molecular weight DNA from an individual with one red and one green pigment gene (1:1) was prepared and digested as described (8) with *Mlu* (M), *Nru* I (N), and *Bss*H II (B). Samples were fractionated by alternating CHEF gel electrophoresis (7) (200 volts, 23 hours, 1% agarose, 30-second switching interval, 9°C). The DNA was then transferred to Genetran (Plasco) and hybridized with a full-length cDNA encoding the red visual pigment (3).

D. Vollrath and R. W. Davis, Department of Biochemistry, Stanford University School of Medicine, Stanford, CA 94305.

J. Nathans, Howard Hughes Medical Institute, Department of Molecular Biology and Genetics, Johns Hopkins University School of Medicine, Baltimore, MD 21205.

A single band was present after digestion with two of the enzymes, Nru I and BssH II, and these bands are less than 200 kb in size, suggesting that the red and green pigment genes are quite close together. Similar data were obtained with the enzymes Not I, Sac II, and Eag I. If these enzymes are indeed cleaving outside of the red and green pigment gene cluster, then the size of the fragments they produce should be a function of the number of genes possessed by an individual; that is, the more genes, the larger the fragment. DNA from five males whose gene number varies from one to five was cleaved with Not I, fractionated, and probed as before (9) (Fig. 2A). Among the enzymes tested, Not I generated the smallest fragment; therefore, differences in fragment sizes among individuals were most clearly seen with this enzyme.

The predicted increase in fragment size with increasing gene number was observed. The size of each fragment was determined with concatamers of phage λ DNA as standards (Fig. 2B). The fragments range in size from 80 to 240 kb. The model predicts a constant size difference between fragments derived from any two individuals who differ by one gene, regardless of the total number of genes. This difference represents the size

of the repeat unit, consisting of a single gene and any duplicated flanking sequences. In agreement with the model, this experiment revealed an increase in fragment size of 39 kb with each additional gene (10).

The model also predicts that an enzyme that cleaves a small number of times per repeat unit should produce two types of fragments—repeat fragments in which both end points lie within repeated sequences and end fragments in which one end point lies in unique DNA. The copy number of the repeat fragments should be a function of the number of repeat units (that is, genes) in an array, while that of the end fragments should not, because every array has only two ends. To test this prediction, DNA from four of the five individuals used in Fig. 1 was cleaved with the enzyme Sfi I, fractionated, and probed with the red pigment cDNA (Fig. 3A).

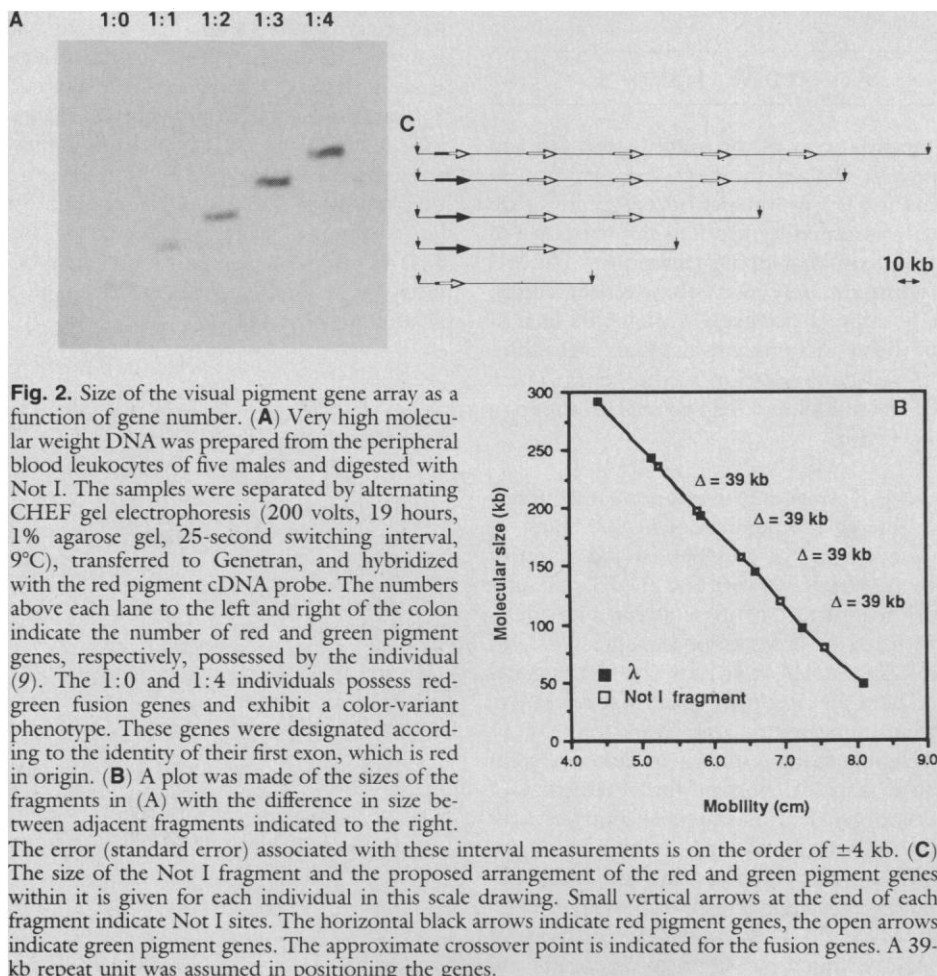
Two classes of bands are present: (i) 3.6-kb and 17-kb bands with intensities that are a function of gene number and (ii) a 32-kb band, the intensity of which is independent of gene number. Upon long exposure, the 3.6-kb band could be seen in all samples, while the 17-kb band was absent from the individual with a single gene. Two Sfi I sites spaced 3.6 kb apart were found at the 3' end

of both the red and green pigment genes in λ genomic clones. These sites bracket the two 3'-most exons of the genes. A probe derived from sequences 3' to these Sfi I sites (Fig. 3B, probe II) (and thus sharing no homology with the cDNA probe) was hybridized to the filter in Fig. 3A after removing the first probe. This second probe detects a different copy number-sensitive 17-kb band in all four samples. The three copy number-sensitive bands (3.6, 17, and 17) thus comprise a total of 37.6 kb, which is very close to the size of the repeat unit determined in Fig. 2.

These data are interpreted as follows and summarized in the restriction map in Fig. 3C. The 3.6-kb band is the same as that observed in genomic clones. The 32-kb band corresponds to the 5' end fragment of the array, because the cDNA probe that detects it extends 5' but not 3' from the 3.6-kb fragment. Similarly, the copy number-sensitive 17-kb band detected by this probe must also be largely derived from 5' sequences. The absence of this 17-kb fragment in the individual with one gene indicates that it spans the boundary between two repeat units. In contrast, the 17-kb fragment detected by the 3' probe (probe II) is present in the individual with one gene, and therefore lies entirely within the repeat unit. The 3' end fragment of the array is not detected with these probes, because it is separated from them by one or more Sfi I sites. These Sfi I digestion data are consistent with a head-to-tail arrangement of the red and green pigment genes (Fig. 3C).

A third prediction of the model is that the red pigment gene lies at the 5' end of the array. To test this, a probe derived from sequences immediately 5' of the red pigment gene and lacking homology to the green pigment gene (Fig. 3B, probe I) was hybridized to an Sfi I digest of DNA from an individual with one red and two green pigment genes. The probe hybridizes specifically to the same 32-kb Sfi I fragment visualized with the cDNA probe (Fig. 4). Moreover, this fragment was cleaved by Not I, which only cuts outside of the array, to produce an 18-kb fragment. Similar results were obtained with DNA from the individual with a single gene. The 5' Not I site can therefore be located relative to the Sfi I sites and the array of genes positioned within the Not I fragments defined in Fig. 2 (Fig. 3C). Because a red pigment gene-specific 5' probe hybridized to the 32-kb 5' end fragment, this gene must be at the 5' end of the array. The third prediction of the model is thus fulfilled.

This report provides compelling physical evidence in support of a model whereby unequal but homologous recombination



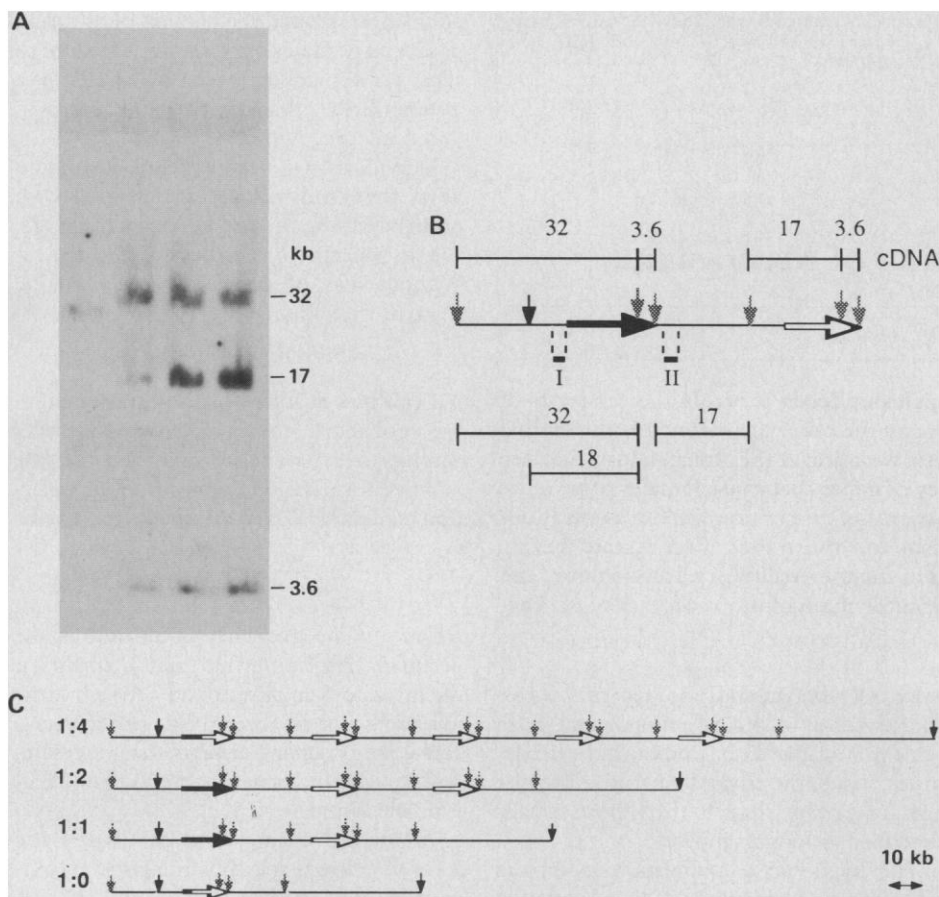


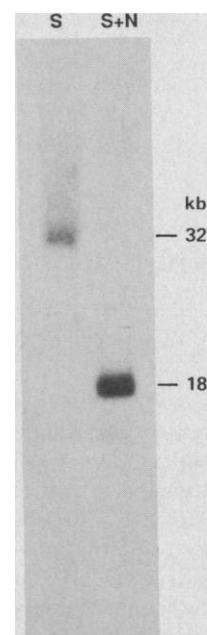
Fig. 3. Sfi I analysis of the visual pigment gene array. **(A)** DNA from four of the five individuals used in Fig. 2 was digested with Sfi I, separated by CHEF gel electrophoresis (200 volts, 18 hours, 1% agarose gel, 2.2-second switching interval, 9°C), transferred to Genetran, and hybridized with the red pigment cDNA probe. Fragment sizes were determined with Bethesda Research Laboratories 1-kb ladder and high molecular weight standards. The largest band in the 1:0 sample is about 2 kb smaller than that in the other samples because the red-green fusion gene in this subject contains the smaller green pigment gene first intron (10). The 5'-most genes of the other individuals contain red pigment gene first introns. **(B)** The fragments visualized in Figs. 3 and 4 and the probes used to detect them are illustrated in this diagram. The red and green pigment genes are as in Fig. 2. The stippled arrows represent Sfi I sites, the vertical black arrow represents the same 5' Not I site as in Fig. 2. Fragments detected by the red pigment cDNA are shown above the arrows. Those detected by probes I and II are shown below the arrows. Probe I (see Fig. 4) is a 0.5-kb Hind III–Bam HI fragment from gJHN33 (3). Probe II is a 1.8-kb Hind III–Eco RI fragment from gJHN53 (3). **(C)** An Sfi I restriction map of the visual pigment gene array in four individuals was constructed with the information in (A). Designations of restriction sites and genes are as in (B) and Fig. 2. A 37.6-kb repeat unit was assumed to build the map.

generates (i) the variation in green but not red pigment gene number observed in normal individuals and (ii) the gene fusions and deletions observed in color-blind individuals. Examples similar to this exist in the human genome. A 5-kb repeat unit containing a λ light chain constant gene varies in number from one to four between individuals (11). Duplication and deletion events at the 21-hydroxylase locus can be explained by unequal homologous recombination in the small two-gene array (12). Lepore hemoglobins are produced from hybrid genes that arose by homologous recombination in the globin gene cluster (13). In none of these systems, however, is the extent and degree of homology as great as at the visual pigment loci.

The high prevalence of red-green color

blindness among humans most likely reflects both an absence of selective pressure and a propensity for the red and green pigment genes to undergo unequal homologous recombination. The latter is a consequence of the gene duplication that occurred some 40 million years ago in the Old World primate lineage (3, 14). Sequence divergence between the duplicated visual pigment genes gave rise to trichromatic vision, while the head-to-tail tandem arrangement provided a substrate for future duplications and deletions. The frequency of homologous rearrangements may be further enhanced by the location of these genes near the end of the long arm of the X chromosome. Recombination events appear to be more frequent both near the ends of chromosomes and in females, where exchanges between X chro-

Fig. 4. A red pigment gene-specific probe hybridizes to the 5' end fragment. DNA from a 1:2 individual (9) was cleaved with either Sfi I (S) or Sfi I and Not I (S + N) and subjected to conventional electrophoresis in a 0.5% agarose gel. Samples were hybridized with red pigment gene-specific probe I (see Fig. 3B), after transfer to Genetran. The double-digest data were used to position the Not I site relative to the two 5'-most Sfi I sites in Fig. 3, B and C.



mosomes occur (15, 16). The present-day variation in these genes provides a pool of visual pigments with altered spectral sensitivities that may represent the first step in the evolution of tetrachromatic vision.

REFERENCES AND NOTES

1. V. A. McKusick, *Mendelian Inheritance in Man* (Johns Hopkins Univ. Press, Baltimore, MD, 1986), p. 1340.
2. J. Nathans *et al.*, *Science* **232**, 203 (1986).
3. J. Nathans *et al.*, *ibid.*, p. 193.
4. J. Gitschier *et al.*, *Nature* **315**, 427 (1985).
5. R. Rozen, J. Fox, W. A. Fenton, A. L. Horwich, L. E. Rosenberg, *ibid.* **313**, 815 (1985).
6. T. P. Yang *et al.*, *ibid.* **310**, 412 (1984).
7. G. Chu, D. Vollrath, R. W. Davis, *Science* **234**, 1582 (1986).
8. D. Vollrath and R. W. Davis, *Nucleic Acids Res.* **15**, 7865 (1987).
9. The number and structure of red and green pigment genes in each of the individuals in this study was determined in (2) and (3). The individuals in Figs. 1, 2, and 3 with red:green pigment gene ratios of 1:0, 1:1, 1:2, 1:3, and 1:4 are numbered 29, 9, 10, 6, and 43, respectively, in (2) and (3). The individual in Fig. 4 is number 14 in (2) and (3).
10. The lengths of the red and green pigment genes are 15.2 kb and 13.3 kb, respectively. The difference results from an insertion of sequences in the first intron of the red pigment gene. The 1:0 individual possesses a red-green fusion gene in which the first intron lacks this insertion because the cross over point between red and green pigment genes occurred very near the 5' end. In terms of gene length, this individual is identical to one with a single green pigment gene. The first interval (1:0 to 1:1) thus represents the size of a red pigment gene repeat unit, while the others represent green pigment gene repeat units.
11. R. A. Taub *et al.*, *Nature* **304**, 172 (1983).
12. P. C. White, M. I. New, B. Dupont, *N. Engl. J. Med.* **316**, 1519 (1987); *ibid.*, p. 1580.
13. J. S. Thompson and M. W. Thompson, *Genetics in Medicine* (Saunders, Philadelphia, PA, 1986), p. 87.
14. J. K. Bowmaker, J. D. Mollon, G. H. Jacobs, in *Colour Vision*, J. D. Mollon and L. T. Sharpe, Eds. (Academic Press, New York, 1983), p. 57; M. O. Dayhoff, *Atlas of Protein Sequence and Structure* (National Biomedical Foundation, Washington, DC, 1972), vol. 5.
15. H. Donis-Keller *et al.*, *Cell* **51**, 319 (1987).
16. D. A. Laurie and M. A. Hulten, *Ann. Human Genet.*

Kin Selection and the Evolution of Monogamy

JOEL R. PECK AND MARCUS W. FELDMAN

A two-locus genetic model is studied in which one locus controls the tendency of individuals to act altruistically toward siblings and the other locus controls the mating habits of females. It is demonstrated that genetic variation at the altruism locus is often sufficient to induce an increase in the frequency of genes that cause females to produce all of their offspring with a single mate. This occurs because of nonrandom associations that develop between genes that cause altruism and those that affect female mating behavior. The results provide a new explanation for the evolution of monogamy, and they suggest a previously unexplored mechanism for the evolution of a variety of other behavioral traits as well.

RECENT THEORETICAL WORK ON the evolution of altruism between relatives has shown, in general, that altruism between closely related kin is more likely to evolve than altruism between distantly related kin (1, 2). This trend motivates the present work, in which we examine the evolution of monogamy, a trait that can control the relatedness of interacting kin. The mating behavior of numerous mammals, birds, fishes, and crustaceans has been described as monogamous, and monogamy has most often been explained by supposed needs for biparental investment in young, although other explanations have been offered as well (3-7). We analyze here a mathematical model and show that if there is genetically based variation in the propensity to be altruistic toward siblings, then monogamy may increase in frequency even when there is no paternal care and when maternal care ends at parturition.

Our model distinguishes two kinds of adult females: those that mate monogamously and those that mate polygamously. Monogamous females are assumed to choose a mate at random and then produce all of their offspring with that mate. By contrast, polygamous females are assumed to produce each of their offspring with a different randomly selected mate. All of the offspring produced by a female are deposited into what we call an "offspring group." Monogamous females produce offspring groups consisting entirely of full sibs, whereas polygamous mothers produce offspring groups consisting entirely of half sibs. Without affecting the results reported here, the

mates of monogamous mothers may be assumed either to practice monogamy or to remain available to be chosen by other females. Thus, the results apply to a broader class of mating systems than those usually described as monogamous.

The hypothetical population is diploid with discrete generations. Genetic variation is allowed at two autosomal loci, each of which has two alleles. One locus controls altruism, and the other controls monogamy. The alleles at the altruism locus are called *A* and *a*, and the alleles at the monogamy locus are called *M* and *m*. There are ten possible genotypes, enumerated as follows:

<i>AA</i>	<i>Aa</i>	<i>aa</i>	<i>AA</i>	<i>Aa</i>
<i>mm</i>	<i>mm</i>	<i>mm</i>	<i>Mm</i>	<i>Mm</i>
1	2	3	4	5
<i>Aa</i>	<i>aa</i>	<i>AA</i>	<i>Aa</i>	<i>aa</i>
<i>mM</i>	<i>Mm</i>	<i>MM</i>	<i>MM</i>	<i>MM</i>
6	7	8	9	10

The rate of recombination between the loci is denoted by *r*, and the frequency of the *i*th genotype immediately before mating and reproduction is denoted by *u_i*. The frequency of *A* is called *p_A*, and the frequency of *M* called *p_M*.

$p_A = u_1 + u_4 + u_8 + 1/2(u_2 + u_5 + u_6 + u_9)$
and

$p_M = 1/2(u_4 + u_5 + u_6 + u_7) + u_8 + u_9 + u_{10}$

Mothers with the *mm* genotype are assumed to be polygamous. Mothers with the *Mm* and *MM* genotypes are monogamous with probabilities *g₁* and *g₂*, respectively, and are polygamous with probabilities $1 - g_1$ and $1 - g_2$, respectively. The monogamy locus is not expressed in males. For convenience, we assume that $g_1 > 0$ and that the

population size and the number of offspring produced per female are sufficiently large to allow us to ignore stochastic effects. We assume further that the two sexes are produced in equal numbers.

Individuals with genotypes *AA*, *Aa*, and *aa* at the altruism locus are altruists with probabilities *b₁*, *b₂*, and *b₃*, respectively (8). We assume that *b₂* lies between *b₁* and *b₃*. Without loss of generality, this may be written:

$$b_1 > b_3 \quad \text{and} \quad b_1 \geq b_2 \geq b_3 \quad (1)$$

Let *w* be a quantity that is proportional to the probability that a given juvenile will survive to reproductive age. We use the additive formulation common in kin selection models (1, 9) and assume that *w* may be expressed as

$$w = 1 - \delta\gamma + z\beta$$

where *z* is the frequency of altruists in the juvenile's offspring group, and δ equals 1 if the juvenile is an altruist and equals 0 if the juvenile is not an altruist. The parameters β and γ are positive constants that represent, respectively, the benefits and costs of altruism. We assume $\gamma \leq 1$.

Let us first examine the case where the allele *m* is fixed, and thus the population is entirely polygamous ($u_1 + u_2 + u_3 = 1$, $u_i = 0$ for $i > 3$). With methods similar to those of Uyenoyama and Feldman (8), it may be shown that when *m* is fixed, both fixation equilibria ($p_A = 0$ or $p_A = 1$) and polymorphic equilibria ($0 < p_A < 1$) are possible at the altruism locus. Numerical and analytic work indicates that both types of equilibrium can be stable. Additive genetic variance is preserved at polymorphic equilibria.

Next, we ask whether a population that is fixed for *m* and that has achieved a stable equilibrium at the altruism locus can be successfully invaded by *M*. It is simple to show that *p_M* will neither increase nor decrease from any initial value if the population is fixed on *A* or *a*. This is not surprising because, when *A* or *a* is fixed, there are no potential sources of differential fitness among the genotypes that have nonzero frequencies.

In contrast to the result for fixation equilibria, when the initial equilibrium at the altruism locus is polymorphic, *M* will always increase to a nonnegligible frequency after invasion (10). On intuitive grounds, it seems likely that these successful invasions by *M* will lead to a subsequent increase in *p_A*. Although analytic proof of this point has eluded us, an extensive numerical study provides strong support for the idea. Parameters were generated randomly for each of 10,000 computer trials. During each trial,